Cytokine Signaling Protein 3 (SOCS3) deficiency in myeloid cells promotes retinal degeneration and angiogenesis through arginase-1 up-regulation in experimental autoimmune uveoretinitis

Accepted Manuscript

SOCS3 deficiency in myeloid cells promotes retinal degeneration and angiogenesis through arginase-1 up-regulation in experimental autoimmune uveoretinitis

Mei Chen, Jiawu Zhao, Imran HA. Ali, Stephen Marry, Josy Augustine, Mohajeet Bhuckory, Aisling Lynch, Adrien Kissenpfennig, Heping Xu

PII: S0002-9440(17)30173-6

DOI: 10.1016/j.ajpath.2017.12.021

Reference: AJPA 2837

To appear in: *The American Journal of Pathology*

Received Date: 2 February 2017

Revised Date: 14 November 2017

Accepted Date: 7 December 2017

Please cite this article as: Chen M, Zhao J, Ali IH, Marry S, Augustine J, Bhuckory M, Lynch A, Kissenpfennig A, Xu H, SOCS3 deficiency in myeloid cells promotes retinal degeneration and angiogenesis through arginase-1 up-regulation in experimental autoimmune uveoretinitis, *The American Journal of Pathology* (2018), doi: 10.1016/j.ajpath.2017.12.021.

SOCS3 deficiency in myeloid cells promotes retinal degeneration and angiogenesis through arginase-1 up-regulation in experimental autoimmune uveoretinitis

Running title: Arginase-1 in EAU-induced angiogenesis

Mei Chen, Jiawu Zhao, Imran HA. Ali, Stephen Marry, Josy Augustine, Mohajeet Bhuckory, Aisling Lynch, Adrien Kissenpfennig, Heping Xu

Centre for Experimental Medicine, School of Medicine, Dentistry & Biomedical Science, Queen's University Belfast, Belfast, UK

Footnote: M.C. and J.Z. contributed equally.

Address correspondence to Heping Xu, The Wellcome-Wolfson Institute of Experimental Medicine, Queen's University Belfast, 97 Lisburn Road, Belfast, BT9 7BL, UK. Tel: 44(0)289097 6463. Email: heping.xu@qub.ac.uk

Funding: Supported by National Eye Research Centre (SCAID061 to H.X.) and Fight for Sight (1361/2 to H.X. and M.C.).

Disclosures: None declared.

Abstract

The suppressor of cytokine signalling protein 3 (SOCS3) critically controls immune cell activation, although its role in macrophage polarization and function remains controversial. Using experimental autoimmune uveoretinitis (EAU) as a model, we show that inflammation-mediated retinal degeneration is exaggerated and retinal angiogenesis is accelerated in mice with SOCS3 deficiency in myeloid cells ($LysM^{Cre/+}SOCS3^{fl/fl}$). At the acute stage of EAU, the population of infiltrating neutrophils was increased and the population of macrophages decreased in $LysM^{Cre/+}SOCS3^{fl/fl}$ mice compared to that in WT mice. Real-time reverse transcription-PCR showed that the expression of tumor necrosis factor-α, IL-1β, interferon-γ, granulocyte-macrophage colony-stimulating factor, and Arginase-1 was significantly higher in the $LysM^{Cre/+}SOCS3^{fl/fl}$ EAU retina in contrast to WT EAU retina. The percentage of Arginase-1^{+} infiltrating cells was significantly higher in the $LysM^{Cre/+}SOCS3^{fl/fl}$ EAU retina than that in the WT EAU retina. In addition, bone-marrow–derived macrophages and neutrophils from the $LysM^{Cre/+}SOCS3^{fl/fl}$ mice express significantly higher levels of CCL2 and Arginase-1 compared to those from WT mice. Inhibition of Arginase using an L-arginine analog amino-2-borono-6-hexanoic suppressed inflammation-induced retinal angiogenesis without affecting the severity of inflammation. Our results suggest that SOCS3 critically controls the phenotype and function of macrophages and neutrophils under inflammatory conditions and loss of SOCS3 promotes the angiogenic phenotype of the cells through up-regulation of Arginase-1.

Introduction

Inflammation-induced angiogenesis is involved in many pathological conditions, including cancer and autoimmune diseases[1-3]. Although the management of angiogenic diseases has been revolutionized over the past decade with the use of VEGF inhibitors[4-6], they remain a major challenge in modern medical care. Previously we reported that chronic inflammation in experimental autoimmune uveoretinitis (EAU) induces retinal angiogenesis[7], a condition mirroring retinal neovascular membrane (RNM) secondary to long-standing posterior segment intraocular inflammation[8] or retinal angiomatous proliferation in age-related macular degeneration[9]. It was further shown that $CCR2^+$ macrophages are critically involved in EAU-induced retinal angiogenesis[7, 10], although the underlying mechanism remains poorly defined.

The EAU retina is characterized by a diverse immune cell infiltrate, including macrophages, neutrophils, dendritic cells, CD4 and CD8 T cells, B cells, and myeloid-derived suppressor cells (MDSC) [10]. The constitution of different subsets of infiltrating cells differs at different stages of EAU. For example, macrophages and neutrophils constitute 40% and 10% of retinal infiltrating cells during acute EAU (ie, day 25 post-immunization (p.i.)), and are reduced to 19% and 1%, respectively, during latter chronic stages of EAU[10]. On the other hand, the percentage of CD8 T cells, CD11c dendritic cells, and MDSCs increased from the acute stage to the chronic stage[10]. Furthermore, a dynamic change in the phenotype of the infiltrating cells in different stages of EAU was also observed. For instance, the majority of macrophages were found to be $CD68^+$ (proinflammatory phenotype) during the acute stages, whereas at the chronic (angiogenic) stages, over half of the infiltrating F4/80 macrophages were found to be Arginase-1^+ (wound-healing phenotype)[7]. These results suggest that the microenvironment of the inflamed retina not only controls the type of circulating immune cells to be recruited but also determines the phenotype and function of infiltrating cells.

CCL2/CCR2 but not CX3CL1/CX3CR1 pathway is critically involved in the trafficking of monocytes across the blood retinal barrier in EAU[11], although in the absence of the CCL2/CCR2 pathway, neutrophils can infiltrate the retina and induce inflammation. In the inflamed retina, infiltrating immune cells respond to environmental cues through cell surface receptors and differentiate into different types of effector cells. The JAK/STAT pathways are critically involved in many cytokine receptor signalling cascades[12]. Although, there are only four known JAKs and seven STATs, collectively they control over 40 cytokine receptor signalling [12, 13]. The JAK1,2/STAT3 is known to be important for the transduction and transcription of cytokines involved in proliferation and angiogenesis such as IL-6, vascular endothelial growth factor (VEGF), epidermal growth factors, and granulocyte-macrophage colony-stimulating factor (GM-CSF)[12, 14, 15]. The SOCS proteins negatively regulate the JAK/STAT pathways through association with key phosphorylated tyrosine residues on JAK and/or cytokine receptors[16]. SOCS3 critically control the JAK1,2/STAT3 pathway [17-19]. The role of SOCS3 in macrophage polarization and function remains controversial[20, 21].

This study aimed to understand the role of SOCS3 in myeloid cell activation and function in the context of EAU. We show that EAU-induced retinal degeneration was exaggerated and angiogenesis was accelerated in the myeloid-cell–specific SOCS3 deficient mice (ie, $LysM^{Cre/+}SOCS3^{fl/fl}$ mice). Further mechanistic studies highlighted that deletion of *SOCS3* led to increased Arginase-1 (Arg-1) and CCL2 expression in both macrophages and neutrophils.

Materials and Methods

Mice and induction of experimental autoimmune uveoretinitis

Eight- to 12-week–old C57BL/6J, $SOCS3^{fl/fl}$, and $LysM^{Cre/+}SOCS3^{fl/fl}$ mice (both in C57BL/6J background) were used in the study. The $LysM^{Cre/+}SOCS3^{fl/fl}$ mice were obtained by crossbreeding the $SOCS3^{fl/fl}$ mice and the LysM-Cre mice. The absence of SOCS3 in myeloid

cells in the LysM$^{Cre/+}$SOCS3$^{fl/fl}$ mice was confirmed by Western blotting of peritoneal macrophages. The SOCS3$^{fl/fl}$ mice were used as controls in some experiments. All mice were maintained in the Biological Research Unit at Queen's University Belfast and exposed to 12h-light/12-night cycle with free access to water and food. All procedures were conducted under the regulation of the UK Home Office Animals (Scientific Procedures) Act 1986, and approved by the Animal Welfare & Ethical Review Body of Queen's University Belfast.

EAU was induced in mice using a protocol described previously [22, 23]. Briefly, mice were immunized with 500 µg $IRBP_{1-20}$ (GPTHLFQPSLVLDMAKVLLD, GL Biochem, Shanghai, China), emulsified 1:1 in complete Freund's adjuvant (DIFCO Laboratories, Detroit, MI), and supplemented with 2.5mg/mL *Mycobacterium tuberculosis H37Ra* (DIFCO Laboratories). An additional 1µg of *Bordetella pertussis toxin* (Tocris Bioscience, Bristol, UK) was administered i.p. immediately after immunization injection.

Clinical assessment of retinal inflammation

Retinal inflammation was assessed clinically at different days post-immunization (p.i.) by the Topical Endoscopic Fundus Imaging system and scored using the criteria described previously[24]. The animals were anaesthetized using isoflurane (Merial Animal Health Ltd., Essex, UK), and pupils were dilated with 1% atropine sulphate and 2.5% phenylephrine hydrochloride (Chauvin, Essex, UK). Fundus images were captured by Nikon D90 camera via an endoscope and saved in TIF format. The inflammation score is based on i) the number and size of retinal infiltrates, ii) the severity of optic disc swelling, and iii) the severity and number of vascular cuffing[24]. Whereas the structural damage score is based on the area of retinal lesion or atrophy and the number of linear lesion[24]. Inflammation and structure damage scores were analyzed separately.

Fundus fluorescein angiography (FFA) was conducted by intraperitoneal injection of 100µL 10% sodium fluorescein to mice. The FFA images were recorded within 5 mins using the Spectralis™ HRA2 confocal scanning laser ophthalmoscope (Heidelberg Engineering Ltd., Hertfordshire,

UK). Four images were taken from different regions of the fundus in each eye. The number of localized hyper-fluorescence lesions in each eye were manually counted using the FFA images.

Spectral domain-optical coherence tomography (SD-OCT) imaging

Mice were anaesthetized with Ketamine (Vetoquinol UK Ltd., Buckingham, UK) and Rompun (Bayer Health Care, Kiel, Germany) via intraperitoneal injection. Pupils were dilated as described above. Viscotears Liquid Gel (Novartis Pharmaceuticals Ltd., Surrey, UK) was used to moisture the ocular surface. OCT scans (30º field of view) were conducted using the SD-OCT system (Heidelberg Engineering Ltd., Hertfordshire, UK). Neuroretinal thickness (from nerve fiber layer to RPE) was measured 1000μm distance away from the optical disc at four quadrants.

***In vivo* treatment**

WT EAU mice were administered intraperitoneally with the arginase inhibitor, amino-2-borono-6-hexanoic acid (ABH, 200μM, Cayman Chemical Company, MI) once daily from day 60 to day 79 p.i. The $LysM^{Cre/+}SOCS3^{fl/fl}$ EAU mice were treated with 200 μM ABH from day 14 to day 59 p.i. Clinical and histological examination was conducted at the end of treatment. The control EAU group received 100 μL PBS injections.

Histopathology

Mouse eyes were fixed in 2.5% (w/v) glutaraldehyde (Agar Scientific Ltd., Stansted, UK) for 24h, then embedded in paraffin and processed for H&E staining. Sections from four layers, 100μm apart were studied in each eye and the severity of EAU was graded according to the criteria described previously [25].

Immunofluorescence of Retinal whole-mounts or sections

Mouse eyes were fixed with 2% paraformaldehyde (Agar Scientific Ltd.) at room temperature for 2h. The retinas were dissected and permeabilized with 0.3% Triton X-100 (Sigma-Aldrich, Dorset, UK) in PBS for 6h. The samples were then incubated with rabbit anti-mouse collagen IV

(AbD Serotec, Kidlington, UK), or rat anti-mouse CD45 (BD Biosciences, Oxford, UK) and rabbit anti-arginase-1 (Santa Cruz, Heidelberg, Germany) at 4 ^{o}C overnight, followed by incubating with Alexa Fluor 546–conjugated donkey anti-rabbit IgG or Alexa Fluo 488–conjugated donkey anti-rat IgG (Life Technologies Ltd, Paisley, UK) for 3h. After thorough washes, samples were mounted on glass slides with Vectashield mounting medium (Vector Laboratories, Burlingame, CA).

Retinal cryosections (6μm thickness) were fixed with 2% paraformaldehyde for 30 minutes. Samples were blocked with 10% bovine serum albumin (BSA), followed by incubation with anti-mouse collagen IV (AbD Serotec) and rat anti-mouse CD105 (Bio-Red Laboratories Led, Watford, UK) for 2h. After thorough washes, samples were incubated with Alexa Fluor 488–conjugated donkey anti-rabbit IgG and Alexa Fluor 546–conjugated goat anti-rat IgG (Life Technologies Ltd) for 1h. All samples were examined by confocal microscopy (Eclipse TE200-U, Nikon UK Ltd, Surry, UK).

Cell culture

Bone-marrow–derived macrophages (BMDMs)

Bone marrows were flushed from the tibia and femur of WT and LysM$^{Cre/+}$SOCS3$^{fl/fl}$ mice. Red blood cells were removed with lysis buffer. The cells were then cultured in DMEM (Gibco BRL, Paisley, UK) supplemented with 10% FCS and 15% L929 conditioned medium and 100μg/mL Primocin (InvivoGen, San Diego, CA) at 37 °C for seven days. The BMDMs were harvested and phenotype confirmed by flow cytometry (>95% CD11b^{+}F4/80^{+}). The BMDMs were further stimulated overnight with 100ng/mL IFN-γ (R&D Systems, Abingdon, UK) + 50ng/mL LPS (Sigma-Aldrich) for M1 activation or with 20ng/mL IL-4 (R&D Systems) for M2 activation [26].

Bone marrow neutrophils

Neutrophils were purified from the bone marrow of SOCS3$^{fl/fl}$ and LysM$^{Cre/+}$SOCS3$^{fl/fl}$ mice using a Neutrophil Isolation Kit (Miltenyi Biotec, Bisley, UK) and confirmed to be >90% Ly6G^{+}.

Total RNAs were isolated from the cells and further processed for real-time reverse transcription-PCR analysis of immune-related genes.

Neutrophil oxidative burst assay

Fresh isolated bone marrow neutrophils ($1x10^5$) from WT and LysM-Cre:SOCS3$^{fl/fl}$ mice were mixed with 50μg/mL dihydrorhodamine (DHR) 123 (Life Technologies) in 200μL RPMI1640 supplemented with 10% FCS and 100μg/mL Primocin (InvivoGen) in FACS tubes at 37 ºC for 20mins. The reaction was stopped by cooling samples on ice for 10min. Rhodamine generated from DHR123 by reactive oxygen species was examined by flow cytometry (BD FACSCantoII, BD Biosciences). The data were analyzed by FlowJo Software (TreeStar Inc., OR).

Neutrophil phagocytosis assay

Fresh isolated bone marrow neutrophils ($5x10^4$) were mixed with $1x10^6$ FITC-conjugated E.coli particles in 1mL RPMI1640 supplemented with 10% FCS and 100μg/mL Primocin (InvivoGen) in FACS tubes and incubated at 37 ºC for 2 hr or 24 hr. Samples were rapidly chilled on ice, and free E.coli particles were washed away by ice-cold PBS. Samples incubated at 4 ºC were used as background controls. Samples were examined by BD FACSCantoII (BD Biosciences). The data were analyzed by FlowJo Software (TreeStar Inc., OR).

Flow cytometry

Retinal single cell preparation

The retinas were dissected and treated with 1 mg/mL collagenase I (Sigma-Aldrich) at 37 ^oC for 30mins. The single cell suspension was washed and filtered through a 100 μm cell strainer (BD Biosciences). The cell suspension from one retina was used for each flow cytometry analysis.

Preparation of cells from blood and spleen

Mouse whole blood were collected in heparinized tubes and 30μL were used for FACS staining. The spleen was homogenized and single cell suspension was obtained by passing samples

through a 100μm cell strainer (BD Labware, Oxford, UK). Red blood cells were removed with lysis buffer and $2x10^5$ splenocytes were used for FACS staining.

Preparation of cells from in vitro *cultures*

The cells were dissociated by incubation in cold PBS followed by scraping and flushing. Cell aggregates were dissociated and single cell suspension was obtained by passing the samples through a cell strainer (100μm). 2×10^5 cells were used for each FACS staining.

FACS staining, acquisition, and analysis

After blocking the Fcγ receptor with anti-mouse CD16/CD32 (2.4G2, BD Biosciences) for 15mins, the cells were incubated with fluorochrome-conjugated antibody cocktail (Table 1) for 30mins on the ice. The samples were washed and re-suspended in 200 μL FACS buffer and processed for FACS analysis using the FACS CantoII (BD Biosciences). All data were analyzed using the FlowJo Software (TreeStar Inc., OR). The gating strategy to detect retinal infiltrating immune cells is detailed in our previous publication [10].

Real-Time Reverse Transcription-PCR

The RNeasy Mini Kit (Qiagen, West Sussex, UK) and the TRI Reagent (Sigma-Aldrich) were used to extract total RMA from retinal tissue and cell cultures, respectively. The same amount of total RNA was used for reverse transcription using the SuperScript™ II Reverse Transcriptase kit (Invitrogen, Paisley, UK) according to the manufacturer's instructions. The mRNA expression levels of different genes were quantified by the real-time reverse transcription-PCR using the LightCycler® 480 system with SYBR Green I Master (Roche Diagnostics GmbH, Mannheim, Germany). The primers used are listed in Table 2. 18S was used as a housing-keeping gene. Murine *IL17A* and GMCSF mRNA expression levels were determined with LightCycler® 480 Probe Master (Roche Diagnostics GmbH).

Measurement of cytokine and nitric oxide

Cytokines TNF-α, IL-6, IFN-γ, IL-10, and CCL2 in the supernatants of BMDMs were analyzed using cytometric bead array assay (BD Biosciences) according to the manufacturer's instructions. VEGF-a was measured using the DuoSet ELISA kit (R&D Systems). Nitric oxide (NO) production in the supernatant was assessed using the Griess Reagent Kit (Life Technologies).

Data analysis

All clinical and histological scores were independently graded by two researchers, and the averages of the two scores were used as the final scores for statistical analysis. EAU clinical and histological scores were analyzed by the Mann-Whitney U test. Retinal whole-mount and cell culture data were analyzed by Student's *t*-test. Retinal immune cell infiltration and gene expression at different time points in WT and LysM$^{Cre/+}$SOCS3$^{fl/fl}$ mice were analyzed by two-way ANOVA. All data were presented as mean ± SEM. Probability values of <0.05 were considered as statistically significant.

Results

Retinal inflammation and degeneration in LysM$^{Cre/+}$SOCS3$^{fl/fl}$ EAU mice

Early retinal inflammation was observed at day 11 p.i. in both WT and LysM$^{Cre/+}$SOCS3$^{fl/fl}$ mice, characterized by swelling of the optic disc and vascular cuffing (Fig. 1A). The severity of inflammation was increased at day 14, reached peak at day 25 p.i., and then decreased slightly at day 60 and 90p.i. (Fig. 1A, B). Inflammatory scores of the LysM$^{Cre/+}$SOCS3$^{fl/fl}$ mice were significantly higher than those of WT mice at day 14 p.i. but not at later time points (Fig. 1B). Interestingly, the structural damage characterized by linear lesions (Fig. 1A) and retinal atrophy (Fig. 1A, C), was more severe in LysM$^{Cre/+}$SOCS3$^{fl/fl}$ EAU mice than that in WT EAU mice. A repeated study using C57BL/6 WT, SOCS3$^{fl/fl}$, and LysM$^{Cre/+}$SOCS3$^{fl/fl}$ mice confirmed that the

LysM$^{Cre/+}$SOCS3$^{fl/fl}$ mice suffered from more severe EAU-mediated retinal damage compared to WT mice, and there was no difference between SOCS3$^{fl/fl}$ and WT EAU mice (Supplementary Figure S1).

Retinal degeneration was further confirmed by SD-OCT examination. The thickness of neuroretina was comparable in non-immunized WT and LysM$^{Cre/+}$SOCS3$^{fl/fl}$ mice. Following EAU induction, although the thickness was progressively reduced in both WT and LysM$^{Cre/+}$SOCS3$^{fl/fl}$ mice, the reduction was more pronounced in the LysM$^{Cre/+}$SOCS3$^{fl/fl}$ EAU mice particularly at day 25 p.i. (Supplementary Figure S2).

Histological examination showed that cell infiltration in WT and LysM$^{Cre/+}$SOCS3$^{fl/fl}$ mice at day 25 and day 90 p.i. was comparable (Fig. 1D, 1E). However, the LysM$^{Cre/+}$SOCS3$^{fl/fl}$ EAU mice displayed higher levels of structural damage, characterized by the disappearance of photoreceptors, disarrangement of retinal layers, and appearance of subretinal/intraretinal scars compared to WT EAU mice (Fig. 1D, 1E). Taken together, these results suggest that deletion of SOCS3 in myeloid cells resulted in severe retinal degeneration in our model of EAU.

Early onset of retinal angiogenesis in LysM$^{Cre/+}$SOCS3$^{fl/fl}$ EAU mice

FFA showed normal retinal vasculature in non-immunized WT and LysM$^{Cre/+}$SOCS3$^{fl/fl}$ mice (Fig. 2A). Small patches of hyper-fluorescein lesions (an indication of localized severe vascular abnormality) were observed at day 60 p.i. WT mice. However, in LysM$^{Cre/+}$SOCS3$^{fl/fl}$ EAU mice, similar lesions were observed as early as at day 25 p.i. (Fig. 2A). The number and size of the lesion increased as the disease progressed in both WT and LysM$^{Cre/+}$SOCS3$^{fl/fl}$ mice (Figs. 2A, 2B). Significantly more lesions were observed in LysM$^{Cre/+}$SOCS3$^{fl/fl}$ EAU mice at day 60 and 90 p.i., compared to WT EAU mice (Figs. 2A, 2B).

Confocal microscopy of retinal flatmounts detected patches of collagen IV^{+} lesions that contain area of diffuse collagen deposition and new blood vessels (Fig. 2C). The new blood vessels were further confirmed by collagen IV and CD105 dual staining (Fig. 2D). The results suggest the

fibro-vascular nature of the RNM. The LysM$^{Cre/+}$SOCS3$^{fl/fl}$ EAU mice developed the RNM earlier and larger in size compared to WT EAU mice (Fig. 2C, 2D). The data suggest that deletion of SOCS3 in myeloid cells resulted in early onset and more severe retinal fibro-vascular membrane in EAU.

Increased neutrophils in the LysM$^{Cre/+}$SOCS3$^{fl/fl}$ EAU mice

Flow cytometry analysis revealed no difference in the percentage of different subsets of leukocytes (CD4, CD8, CD11b, F4/80, CD11b^{+}Gr1^{+}Ly6G^{+}, CD11b^{+}Gr1^{+}Ly6G^{-}) in the blood and spleen between non-immunized WT and LysM$^{Cre/+}$SOCS3$^{fl/fl}$ mice (Supplementary Figures S3A, S3B). Following induction of EAU, there was a reduction in CD4 and CD8 T cell populations and an increase in CD11b, CD11b^{+}Gr1^{+}Ly6G^{+} (neutrophil), and CD11b^{+}Gr1^{+}Ly6G^{-} MDSC at days 25 and 90 p.i., in the blood (Supplementary Figures S3C) and spleen (data not shown) in both WT and LysM$^{Cre/+}$SOCS3$^{fl/fl}$ mice. However, significantly higher percentages of neutrophils and lower percentages of F4/80^{+} macrophages were observed in LysM$^{Cre/+}$SOCS3$^{fl/fl}$ EAU mice at day 25 p.i. (Supplementary Figures S3C).

Retinal resident microglia are CD45^{int}CD11b^{+} and infiltrating leukocytes are CD45^{hi} [10]. EAU increased the percentages and the absolute number of microglia and infiltrating leukocytes in both WT and LysM$^{Cre/+}$SOCS3$^{fl/fl}$ mice (Figs 3A, 3B). The percentages and absolute numbers of microglia and infiltrating leukocytes were comparable in WT and LysM$^{Cre/+}$SOCS3$^{fl/fl}$ EAU mice. Further analysis of retinal infiltrating leukocyte subsets showed that the LysM$^{Cre/+}$SOCS3$^{fl/fl}$ EAU mice contained more lymphocytes (T/B cells) and less myeloid-derived cells compared to WT EAU mice, particularly at day 90 p.i. (Figs. 3C, 3D). Within the myeloid-derived cells, higher percentages of neutrophils were observed in the LysM$^{Cre/+}$SOCS3$^{fl/fl}$ EAU retina at both day 25 and 90 p.i. (Figs. 3C, 3D). These results suggest that deletion of SOCS3 in myeloid cells shifts retinal immune infiltration towards lymphocytes and neutrophils in EAU.

Inflammatory and angiogenic gene expression in EAU mouse retina

Under non-inflammatory condition, the LysM$^{Cre/+}$SOCS3$^{fl/fl}$ mouse retina expressed significantly higher levels of TNF-α, iNOS, GM-CSF, VEGFa, and Arg-1 compared to WT mouse retina (Fig. 4A). The expression of IFNγ, IL-17a, IL-10, and IL-6 was below detectable levels in both WT and LysM$^{Cre/+}$SOCS3$^{fl/fl}$ mice. After EAU induction, the expression of iNOS, TNF-α, IL-1β, GM-CSF, IFN-γ, IL-17a, IL-6, IL-10, CXCL2, and CCL2 was markedly increased at day 25 p.i. and remained at high levels throughout the course of the study in both WT and LysM$^{Cre/+}$SOCS3$^{fl/fl}$ mice (Fig 4B). The LysM$^{Cre/+}$SOCS3$^{fl/fl}$ EAU retina expressed significantly higher levels of TNF-α, IL-1β, GM-CSF, IFN-γ, IL-6, CCL2, CXCL2, and VEGFa compared to the WT EAU retina (Fig 4B). Importantly, the expression level of Arg-1 in the LysM$^{Cre/+}$SOCS3$^{fl/fl}$ EAU mouse was 49-folds higher than that in WT mouse retina at day 25 p.i. (685 ± 218 vs 14 ± 2.7). Retinal whole-mount staining showed that arginase-1 was expressed exclusively in infiltrating CD45^{+} cells (Fig. 4C, 4D), and the percentage of arginase-1^{+} cells was significant higher in LysM$^{Cre/+}$SOCS3$^{fl/fl}$ EAU retina (35%, Fig. 4D) compared to WT EAU retina (18%, Fig. 4C). These results suggest that the LysM$^{Cre/+}$SOCS3$^{fl/fl}$ EAU retinas expressed higher levels of inflammatory cytokines as well as higher levels of angiogenic growth factors.

The effects of SOCS3 deletion in bone-marrow–derived macrophages and neutrophils

Using a standard BMDM culture protocol, similar numbers of F4/80^{+}CD11b^{+} cells were yielded from LysM$^{Cre/+}$SOCS3$^{fl/fl}$ and SOCS3$^{fl/fl}$ mice, suggesting that deletion of SOCS3 in myeloid lineage did not affect macrophage differentiation. Naïve SOCS3-deficient BMDMs expressed higher levels of IL-1β, VEGFa, and Arg-1 compared to WT cells (Fig. 5A). Following LPS/IFN-γ stimulation, the expression of inflammatory genes including *TNFA*, *IL1β, iNOS*, and *IL6* was significantly increased in both SOCS3$^{fl/fl}$ and SOCS3-deficient cells (data not shown). Interestingly, higher levels of *IL10* mRNA were observed in SOCS3-deficient BMDMs (Fig. 5B). IL-4 treatment increased the expression of IL-10, CCL2, VEGF, Ym-1, and Arg-1 in both

SOCS3$^{fl/fl}$ and SOCS3-deficient BMDMs (data not shown), although the expression of CCL2 and Arg-1 was significantly higher in SOCS3-deficient BMDMs compared to SOCS3$^{fl/fl}$ BMDMs (Fig. 5C). Neutrophils from SOCS3-deficient mice expressed significantly higher levels of Arg-1, CCL2, and IL-6 compared to those from WT mice (Fig. 5D). The oxidative burst and phagocytic activity was also higher in SOCS3-deficient neutrophils (Supplementary figure S4).

SOCS3-deficient BMDM produced higher levels of VEGF (under non-stimulatory conditions), IL-10 (after IFNγ/LPS stimulation), and CCL2 (after IL-4 stimulation) compared to SOCS3$^{fl/fl}$ BMDMs (Fig. 5E). The production of TNF-α, IL-6, IFNγ, and NO did not differ between groups (Fig. 5E).

The effect of arginase inhibition in inflammation-induced retinal angiogenesis

To determine whether the early onset and severe RNM in LysM$^{Cre/+}$SOCS3$^{fl/fl}$ EAU retinas was due to enhanced Arg-1 expression, LysM$^{Cre/+}$SOCS3$^{fl/fl}$ EAU mice were treated with an arginase inhibitor (ABH) from day 14 to 59 p.i. Although the severity of inflammation remained unaffected (Fig. 6A), retinal structure damage (Fig. 6A) and angiogenesis (Fig. 6B) was significantly reduced in ABH-treated mice compared to PBS controls.

The WT EAU mice develop RNM at day 60 p.i., the mice were therefore treated with ABH from day 60 ~ 79 p.i. The treatment did not affect the severity of inflammation and structural damage (Fig. 6C), but reduced the overall area of RNM (Fig. 6D) and the number localized hyper-fluorescein lesion in FFA (Fig. 6E). The results suggest that arginase activity may critically contribute to EAU-induced RNM.

Discussion

This study shows that the deletion of SOCS3 in myeloid cells resulted in severe retinal degeneration and an early onset of retinal fibrovascular membrane in EAU. It further shows that

the LysM$^{Cre/+}$SOCS3$^{fl/fl}$ EAU retina expressed higher levels of inflammatory cytokines (IL-1β, TNFα, and IFNγ) and angiogenic growth factors (VEGF and Arg-1) compared to WT EAU retina. Deletion of SOCS3 increased the expression of Arg-1 in macrophages and neutrophils. Importantly, it shows that the inhibition of arginase in EAU reduced retinal fibrovascular membrane without affecting the severity of inflammation. These results implicate a role for SOCS3 in regulating the phenotype and function of myeloid cells in retinal inflammation.

Retinal degeneration in EAU is primarily caused by antigen-specific T-cell–mediated photoreceptor death[27, 28], although inflammatory mediators such as TNF-α, IL-1β, reactive oxygen/nitric species (eg, NO) released by infiltrating neutrophils and macrophages also critically contribute to retinal cell death [29-31]. The total number of retinal infiltrating cells was comparable between WT and LysM$^{Cre/+}$SOCS3$^{fl/fl}$ EAU mice, but the latter displayed more lymphocytes and neutrophils and fewer macrophages. Previous studies in EAE [32] and arthritis [33] also reported increased neutrophilic infiltration in LysM$^{Cre/+}$SOCS3$^{fl/fl}$ mice. Neutrophil-dominated EAU has been observed in the CCL2 or CCR2 knockout mice by us and others [7, 10], although such inflammation did not cause more severe retinal degeneration compared to the macrophage-dominated EAU in WT mice[7, 10, 34]. The results suggest that the phenotype of infiltrating neutrophils may determine the level of retinal damage. The GM-CSF signaling pathway critically controls neutrophil differentiation and activation, and is negatively regulated by SOCS3[35]. The LysM$^{Cre/+}$SOCS3$^{fl/fl}$ EAU retina expressed higher levels of GM-CSF, and neutrophils from these mice expressed more IL-6, CCL2, and Arg-1, and displayed higher levels of oxidative burst and increased phagocytosis compared to the cells from WT mice. SOCS3 is known to negatively control macrophage phagocytosis and SOCS3 knockdown increases macrophage phagocytic activity [36]. Our results suggest that deletion of SOCS3 may lead to altered neutrophil/macrophage activation, which may contribute to increased retinal degeneration in LysM$^{Cre/+}$SOCS3$^{fl/fl}$ EAU mice.

The higher percentages of infiltrating lymphocytes (CD4, CD8, and B cells) may also contribute to increased retinal degeneration in the LysM$^{Cre/+}$SOCS3$^{fl/fl}$ EAU mice. T-cell activation in autoimmunity is induced by antigen presenting cells, ie, DCs and macrophages, and SOCS3 is known to be critically involved in DC differentiation and functions[37, 38]. SOCS3 can regulate indoleamine 2,3-dioxygenase expression in DCs[39], which critically controls the balance between T-cell activation and tolerance. Over-expression of SOCS3 in DCs suppresses invariant natural killer T-cell activation in autoimmune arthritis[40]. However, a previous study reported reduced potential to drive T effector cell responses and increased induction of tolerogenic T cells by SOCS3 deficient DCs [41], which does not support enhanced autoimmune pathology in the mice observed by us and others. How T-cell activation and migration in EAU is affected in LysM$^{Cre/+}$SOCS3$^{fl/fl}$ mice warrants further investigation.

Macrophages are known to play an important role in retinal degeneration and angiogenesis. Although the percentage of infiltrating macrophages was lower in LysM$^{Cre/+}$SOCS3$^{fl/fl}$ EAU mice compared to that in WT EAU mice, they may be more angioegenic. Macrophage polarization and function are regulated by SOCS proteins, particularly SOCS1 and SOCS3 [21, 42]. For example, SOCS3 negatively regulates GM-CSF–induced CCL2, Arg-1, and MMP-12 expression in BMDMs [43][35]. The higher levels of GM-CSF in LysM$^{Cre/+}$SOCS3$^{fl/fl}$ mouse retina may induce CCL2 and Arg-1 expression in macrophages.

The BMDMs from LysM$^{Cre/+}$SOCS3$^{fl/fl}$ mice appear to have an anti-inflammatory or wound healing phenotype bias evidenced by higher levels of IL-10, VEGF, and Arg-1 expression. This result is in line with previous SOCS3 knockdown studies [44, 45] and a study in tumor metastasis in the LysM$^{Cre/+}$SOCS3$^{fl/fl}$ mouse[46]. However, other studies have shown that deletion of SOCS3 in myeloid cells promoted M1 macrophage differentiation, including increased IL-1β, TNFα, iNOS, and decreased IL-10 expression [47, 48], although the expression of Arg-1 and VEGF was not investigated in those studies. What causes the discrepancy remains unknown. The *in vitro* observation in BMDMs matches the neutrophil data as well as the EAU retina gene expression

profile.

The development of RNM in EAU is related to the shift of infiltrating macrophages from $CD68^+$ to $Arg\text{-}1^+$ phenotype [7]. At day 25 p.i., the expression of *Arg1* mRNA in the $LysM^{Cre/+}SOCS3^{fl/fl}$ mouse retina was substantially higher than that in the WT mouse retina, and treatment of EAU with an arginase inhibitor (ABH) suppressed retinal angiogenesis without affecting the severity of inflammation. Macrophages and neutrophils from $LysM^{Cre/+}SOCS3^{fl/fl}$ mice expressed significantly higher levels of Arg-1 and VEGF compared to those from WT mice. Arginase catalyzes the conversion of arginine to ornithine, a precursor of polyamines and collagen, thus contributing to the production of extracellular matrix that supports angiogenesis[50]. Arginase is known to play an important role in regulating inflammation and is involved in vascular complications of retinal disease, including diabetic retinopathy[51, 52] and choroidal neovascularization[53]. Our results highlight the role of Arg-1 as an important angiogenic mediator under inflammatory conditions.

The early onset of RNM in the $LysM^{Cre/+}SOCS3^{fl/fl}$ mice is in line with the previous observation in the laser-induced choroidal neovascularization in these mice [49], where a link between STAT3 activation in circulating immune cells and neovascular age-related macular degeneration was reported. The role of the SOCS3-STAT3 pathway in retinal inflammation and angiogenesis has been observed in a number of studies. Sun et al showed that SOCS3 in retinal neurons and glial cells suppressed VEGF signalling to prevent pathological neovascular growth in mouse model of oxygen-induced retinopathy [54]. Ozawa et al reported enhanced retinal inflammation and photoreceptor degeneration in retina-specific SOCS3 KO mice following LPS stimulation [55]. Further understanding the role of the SOCS3-STAT3 pathway in retinal health and disease may uncover novel target for therapy.

In summary, our study suggests that SOCS3 critically controls the phenotype and functions of macrophages and neutrophils under inflammatory conditions. In the absence of SOCS3,

macrophages and neutrophils express higher levels of Arg-1, CCL2, IL-6, and VEGF and promote angiogenesis. SOCS3 deficiency also enhances phagocytosis and oxidative bursts in neutrophils, which may contribute to exacerbated retinal degeneration in EAU. Targeting SOCS3 may be a novel approach to control inflammation and its related angiogenesis.

Acknowledgements

M.C., J.Z., I.A.H., S.M., and A.L. conducted the experiment. A.K. provided LysM$^{Cre/+}$SOCS3$^{fl/fl}$ mice. M.C. and H.X. designed the experiments, supervised the work, and analyzed the data. J.Z., M.C., and H.X. wrote the manuscript. All the authors have read the manuscript and approve the submission.

References

1. Marrelli A, Cipriani P, Liakouli V, Carubbi F, Perricone C, Perricone R, Giacomelli R: Angiogenesis in rheumatoid arthritis: a disease specific process or a common response to chronic inflammation? Autoimmun Rev 2011, 10:595-598.

2. Costa C, Incio J, Soares R: Angiogenesis and chronic inflammation: cause or consequence? Angiogenesis 2007, 10:149-166.

3. Majno G: Chronic inflammation: links with angiogenesis and wound healing. Am J Pathol 1998, 153:1035-1039.

4. Kim LA, D'Amore PA: A brief history of anti-VEGF for the treatment of ocular angiogenesis. Am J Pathol 2012, 181:376-379.

5. Campa C, Harding SP: Anti-VEGF compounds in the treatment of neovascular age related macular degeneration. Curr Drug Targets 2011, 12:173-181.

6. Grothey A, Galanis E: Targeting angiogenesis: progress with anti-VEGF treatment with large molecules. Nat Rev Clin Oncol 2009, 6:507-518.

7. Chen M, Copland DA, Zhao J, Liu J, Forrester JV, Dick AD, Xu H: Persistent inflammation subverts thrombospondin-1-induced regulation of retinal angiogenesis and is driven by CCR2 ligation. Am J Pathol 2012, 180:235-245.

8. Dhingra N, Kelly S, Majid MA, Bailey CB, Dick AD: Inflammatory choroidal neovascular membrane in posterior uveitis-pathogenesis and treatment. Indian J Ophthalmol 2010, 58:3-10.

9. Yannuzzi LA, Negrao S, Iida T, Carvalho C, Rodriguez-Coleman H, Slakter J, Freund KB, Sorenson J, Orlock D, Borodoker N: Retinal angiomatous proliferation in age-related macular degeneration. Retina 2001, 21:416-434.

10. Zhao J, Chen M, Xu H: Experimental autoimmune uveoretinitis (EAU)-related tissue damage and angiogenesis is reduced in CCL2(-)/(-)CX(3)CR1gfp/gfp mice. Invest Ophthalmol Vis Sci 2014, 55:7572-7582.

11. Chen M, Zhao J, Luo C, Pandi SP, Penalva RG, Fitzgerald DC, Xu H: Para-inflammation-mediated retinal recruitment of bone marrow-derived myeloid cells following whole-body irradiation is CCL2 dependent. Glia 2012, 60:833-842.

12. O'Shea JJ, Holland SM, Staudt LM: JAKs and STATs in immunity, immunodeficiency, and cancer. N Engl J Med 2013, 368:161-170.

13. Miklossy G, Hilliard TS, Turkson J: Therapeutic modulators of STAT signalling for human diseases. Nat Rev Drug Discov 2013, 12:611-629.

14. Chen Z, Han ZC: STAT3: a critical transcription activator in angiogenesis. Med Res Rev 2008, 28:185-200.

15. Lu W, Chen H, Yel F, Wang F, Xie X: VEGF induces phosphorylation of STAT3 through binding VEGFR2 in ovarian carcinoma cells in vitro. Eur J Gynaecol Oncol 2006, 27:363-369.

16. Alexander WS, Starr R, Metcalf D, Nicholson SE, Farley A, Elefanty AG, Brysha M, Kile BT, Richardson R, Baca M, Zhang JG, Willson TA, Viney EM, Sprigg NS, Rakar S, Corbin J, Mifsud S, DiRago L, Cary D, Nicola NA, Hilton DJ: Suppressors of cytokine signaling (SOCS): negative regulators of signal transduction. J Leukoc Biol 1999, 66:588-592.

17. Yoshimura A, Yasukawa H: JAK's SOCS: a mechanism of inhibition. Immunity 2012, 36:157-159.

18. Yoshimura A, Suzuki M, Sakaguchi R, Hanada T, Yasukawa H: SOCS, Inflammation, and Autoimmunity. Front Immunol 2012, 3:20.

19. Carow B, Rottenberg ME: SOCS3, a Major Regulator of Infection and Inflammation. Front Immunol 2014, 5:58.

20. Wilson HM: SOCS Proteins in Macrophage Polarization and Function. Front Immunol 2014, 5:357.

21. McCormick SM, Heller NM: Regulation of Macrophage, Dendritic Cell, and Microglial Phenotype and Function by the SOCS Proteins. Front Immunol 2015, 6:549.

22. Avichezer D, Silver PB, Chan CC, Wiggert B, Caspi RR: Identification of a new epitope of human IRBP that induces autoimmune uveoretinitis in mice of the H-2b haplotype. Invest Ophthalmol Vis Sci 2000, 41:127-131.

23. Xu H, Manivannan A, Crane I, Dawson R, Liversidge J: Critical but divergent roles for CD62L and CD44 in directing blood monocyte trafficking in vivo during inflammation. Blood 2008, 112:1166-1174.

24. Xu H, Koch P, Chen M, Lau A, Reid DM, Forrester JV: A clinical grading system for retinal inflammation in the chronic model of experimental autoimmune uveoretinitis using digital fundus images. Exp Eye Res 2008, 87:319-326.

25. Dick AD, Cheng YF, Liversidge J, Forrester JV: Intranasal administration of retinal antigens suppresses retinal antigen-induced experimental autoimmune uveoretinitis. Immunology 1994, 82:625-631.

26. Luo C, Chen M, Madden A, Xu H: Expression of complement components and regulators by different subtypes of bone marrow-derived macrophages. Inflammation 2012, 35:1448-1461.

27. Caspi RR, Roberge FG, Chan CC, Wiggert B, Chader GJ, Rozenszajn LA, Lando Z, Nussenblatt RB: A new model of autoimmune disease. Experimental autoimmune uveoretinitis induced in mice with two different retinal antigens. J Immunol 1988, 140:1490-1495.

28. Liversidge J, Forrester JV: Experimental autoimmune uveitis (EAU): immunophenotypic analysis of inflammatory cells in chorio retinal lesions. Curr Eye Res 1988, 7:1231-1241.

29. Forrester JV, Liversidge J, Dua HS, Dick A, Harper F, McMenamin PG: Experimental autoimmune uveoretinitis: a model system for immunointervention: a review. Curr Eye Res 1992, 11 Suppl:33-40.

30. Dick AD, Ford AL, Forrester JV, Sedgwick JD: Flow cytometric identification of a minority population of MHC class II positive cells in the normal rat retina distinct from CD45lowCD11b/c+CD4low parenchymal microglia. Br J Ophthalmol 1995, 79:834-840.

31. Dick AD, Kreutzer B, Laliotou B, Forrester JV: Phenotypic analysis of retinal leukocyte infiltration during combined cyclosporin A and nasal antigen administration of retinal antigens: delay and inhibition of macrophage and granulocyte infiltration. Ocul Immunol Inflamm 1997, 5:129-140.

32. Qin H, Yeh WI, De Sarno P, Holdbrooks AT, Liu Y, Muldowney MT, Reynolds SL, Yanagisawa LL, Fox TH,3rd, Park K, Harrington LE, Raman C, Benveniste EN: Signal transducer and activator of transcription-3/suppressor of cytokine signaling-3 (STAT3/SOCS3) axis in myeloid cells regulates neuroinflammation. Proc Natl Acad Sci U S A 2012, 109:5004-5009.

33. Wong PK, Egan PJ, Croker BA, O'Donnell K, Sims NA, Drake S, Kiu H, McManus EJ, Alexander WS, Roberts AW, Wicks IP: SOCS-3 negatively regulates innate and adaptive immune mechanisms in acute IL-1-dependent inflammatory arthritis. J Clin Invest 2006, 116:1571-1581.

34. Sonoda KH, Yoshimura T, Egashira K, Charo IF, Ishibashi T: Neutrophil-dominant experimental autoimmune uveitis in CC-chemokine receptor 2 knockout mice. Acta Ophthalmol 2011, 89:e180-8.

35. Tortorella C, Simone O, Piazzolla G, Stella I, Antonaci S: Age-related impairment of GM-CSF-induced signalling in neutrophils: role of SHP-1 and SOCS proteins. Ageing Res Rev 2007, 6:81-93.

36. Gordon P, Okai B, Hoare JI, Erwig LP, Wilson HM: SOCS3 is a modulator of human macrophage phagocytosis. J Leukoc Biol 2016, 100:771-780.

37. Dimitriou ID, Clemenza L, Scotter AJ, Chen G, Guerra FM, Rottapel R: Putting out the fire: coordinated suppression of the innate and adaptive immune systems by SOCS1 and SOCS3 proteins. Immunol Rev 2008, 224:265-283.

38. Liu X, Qu X, Chen Y, Liao L, Cheng K, Shao C, Zenke M, Keating A, Zhao RC: Mesenchymal stem/stromal cells induce the generation of novel IL-10-dependent regulatory dendritic cells by SOCS3 activation. J Immunol 2012, 189:1182-1192.

39. Orabona C, Pallotta MT, Volpi C, Fallarino F, Vacca C, Bianchi R, Belladonna ML, Fioretti MC, Grohmann U, Puccetti P: SOCS3 drives proteasomal degradation of indoleamine 2,3-dioxygenase (IDO) and antagonizes IDO-dependent tolerogenesis. Proc Natl Acad Sci U S A 2008, 105:20828-20833.

40. Veenbergen S, Bennink MB, Affandi AJ, Bessis N, Biton J, Arntz OJ, van den Berg WB, van de Loo FA: A pivotal role for antigen-presenting cells overexpressing SOCS3 in controlling invariant NKT cell responses during collagen-induced arthritis. Ann Rheum Dis 2011, 70:2167-2175.

41. Matsumura Y, Kobayashi T, Ichiyama K, Yoshida R, Hashimoto M, Takimoto T, Tanaka K, Chinen T, Shichita T, Wyss-Coray T, Sato K, Yoshimura A: Selective expansion of foxp3-positive regulatory T cells and

immunosuppression by suppressors of cytokine signaling 3-deficient dendritic cells. J Immunol 2007, 179:2170-2179.

42. Wilson HM: SOCS Proteins in Macrophage Polarization and Function. Front Immunol 2014, 5:357.

43. Jost MM, Ninci E, Meder B, Kempf C, Van Royen N, Hua J, Berger B, Hoefer I, Modolell M, Buschmann I: Divergent effects of GM-CSF and TGFbeta1 on bone marrow-derived macrophage arginase-1 activity, MCP-1 expression, and matrix metalloproteinase-12: a potential role during arteriogenesis. FASEB J 2003, 17:2281-2283.

44. Liu Y, Stewart KN, Bishop E, Marek CJ, Kluth DC, Rees AJ, Wilson HM: Unique expression of suppressor of cytokine signaling 3 is essential for classical macrophage activation in rodents in vitro and in vivo. J Immunol 2008, 180:6270-6278.

45. Arnold CE, Whyte CS, Gordon P, Barker RN, Rees AJ, Wilson HM: A critical role for suppressor of cytokine signalling 3 in promoting M1 macrophage activation and function in vitro and in vivo. Immunology 2014, 141:96-110.

46. Hiwatashi K, Tamiya T, Hasegawa E, Fukaya T, Hashimoto M, Kakoi K, Kashiwagi I, Kimura A, Inoue N, Morita R, Yasukawa H, Yoshimura A: Suppression of SOCS3 in macrophages prevents cancer metastasis by modifying macrophage phase and MCP2/CCL8 induction. Cancer Lett 2011, 308:172-180.

47. Qin H, Holdbrooks AT, Liu Y, Reynolds SL, Yanagisawa LL, Benveniste EN: SOCS3 deficiency promotes M1 macrophage polarization and inflammation. J Immunol 2012, 189:3439-3448.

48. Yan C, Ward PA, Wang X, Gao H: Myeloid depletion of SOCS3 enhances LPS-induced acute lung injury through CCAAT/enhancer binding protein delta pathway. FASEB J 2013, 27:2967-2976.

49. Chen M, Lechner J, Zhao J, Toth L, Hogg R, Silvestri G, Kissenpfennig A, Chakravarthy U, Xu H: STAT3 Activation in Circulating Monocytes Contributes to Neovascular Age-Related Macular Degeneration. Curr Mol Med 2016, 16:412-423.

50. Durante W: Role of arginase in vessel wall remodeling. Front Immunol 2013, 4:111.

51. Patel C, Rojas M, Narayanan SP, Zhang W, Xu Z, Lemtalsi T, Jittiporn K, Caldwell RW, Caldwell RB: Arginase as a mediator of diabetic retinopathy. Front Immunol 2013, 4:173.

52. Narayanan SP, Rojas M, Suwanpradid J, Toque HA, Caldwell RW, Caldwell RB: Arginase in retinopathy. Prog Retin Eye Res 2013, 36:260-280.

53. Liu J, Copland DA, Horie S, Wu WK, Chen M, Xu Y, Paul Morgan B, Mack M, Xu H, Nicholson LB, Dick AD: Myeloid cells expressing VEGF and arginase-1 following uptake of damaged retinal pigment epithelium suggests potential mechanism that drives the onset of choroidal angiogenesis in mice. PLoS One 2013, 8:e72935.

54. Sun Y, Ju M, Lin Z, Fredrick TW, Evans LP, Tian KT, Saba NJ, Morss PC, Pu WT, Chen J, Stahl A, Joyal JS, Smith LE. SOCS3 in retinal neurons and glial cells suppresses VEGF signalling to prevent pathological neovascular growth. Sci Signal 2015, 8(395):ra94.

55. Ozawa Y , Nakao K, Kurihara T, Shimazaki T, Shimmura S, Ishida S, Yoshimura A, Tsubota K, Okano H. Roles of STAT3/SOCS3 pathway in regulating the visual function and ubiquitin-proteasome-dependent degradation of rhodopsin during retinal inflammation. J Biol Chem 2008, 283:24561-70.

Figure legends

Figure 1. Retinal inflammation in WT and LysM$^{Cre/+}$SOCS3$^{fl/fl}$ experimental autoimmune uveoretinitis (EAU) mice. EAU was induced in WT and LysM$^{Cre/+}$SOCS3$^{fl/fl}$ mice and clinical inflammation was examined by fundus imaging at different days after immunization, and histology was conducted on day 25 and 90 post-immunization (p.i.). **A:** Fundus images from WT and LysM$^{Cre/+}$SOCS3$^{fl/fl}$ mice on different days after immunization. OD - optic disc; arrows – retinal infiltrates; arrowheads – vascular cuffings. **B:** Clinical score of retinal inflammation. **C:** Clinical score of retinal structure damage at different stages of EAU. N = 6~12, *P < 0.05. Mann Whitney test. **D:** Representative images of H&E staining of EAU retina from WT and LysM$^{Cre/+}$SOCS3$^{fl/fl}$ mice. Small arrows – retinal fulds; large arrows – fibrotic lesions; asterisk – granular lesion. Scale bar = 50 μm. **E, F:** Histological scores on retinal immune cell infiltration and structure damage in WT and LysM$^{Cre/+}$SOCS3$^{fl/fl}$ EAU mice. N = 6, *P < 0.05 compared to WT mice. Mann Whitney test.

Figure 2. Retinal fibrovascular membrane in WT and LysM$^{Cre/+}$SOCS3$^{fl/fl}$ experimental autoimmune uveoretinitis (EAU) mice. EAU was induced in WT and LysM$^{Cre/+}$SOCS3$^{fl/fl}$ mice and fluorescein angiography (FA) was conducted at different days after immunization. **A:** Representative FA images from WT and LysM$^{Cre/+}$SOCS3$^{fl/fl}$ mice on different days after immunization. Arrows indicate the hyper-fluorescent lesions. Scale bar = 500 μm. **B:** The number of hyper-fluorescent lesions per eye in each groups at different times. **C:** Confocal image from a day 60 p.i. WT EAU retina stained for collagen IV showing new blood vessels (arrows) and collagen deposition (asterisk) around a diseased venule. Scale bar = 50 μm. **D:** Confocal image from a retinal section from a day 90 p.i. WT EAU retina stained for collagen IV (green) and CD105 (red) showing multiple vessels (arrows) in retinal fibrovascular membrane. **E, F:** Retinal flatmounts from day 25 and 90 p.i., EAU mice were stained for collagen IV, and imaged by confocal microscopy. Scale bar = 25μm. **E:** Representative images of retinal flatmounts from WT and LysM$^{Cre/+}$SOCS3$^{fl/fl}$ mice showing retinal vasculature and neovascular membrane (arrows). **F:** The size of retinal neovascular membrane in WT and LysM$^{Cre/+}$SOCS3$^{fl/fl}$ mice at day 25 and 90 p.i. N = 6 ~ 8, *P < 0.05 compared to WT mice at the same time point.

Figure 3. The constitution of immune cells in WT and LysM$^{Cre/+}$SOCS3$^{fl/fl}$ experimental autoimmune uveoretinitis (EAU) retina. Retinas from days 25 and 90 p.i. WT and SOCS3 KO mice were collected. Single-cell suspension was prepared (*Materials and Methods*) and stained

for different cell-surface markers and analyzed by flow cytometry. **A:** The percentage and number of retinal microglia cells in different stages of EAU in WT and LysM$^{Cre/+}$SOCS3$^{fl/fl}$ mice. **B:** The percentage and number of retinal infiltrating cells in different stages of EAU in WT and LysM$^{Cre/+}$SOCS3$^{fl/fl}$ mice. Data are presented as mean ± SEM. N = 3. **C, D:** Pie charts showing the percentages of macrophages (F4/80$^+$), neutrophils (CD11$^+$Gr-1$^+$Ly6G$^+$), DCs (CD11c$^+$), MDSCs (CD11b$^+$Gr-1$^+$Ly6G$^-$), B cells (B220$^+$), and CD4$^+$ and CD8$^+$ cells in WT and SOCS3 KO EAU retinas at days 25 (**C**) and 90 (**D**) p.i. Data in pie charts are the means of three mice. *P < 0.05; **P < 0.01, ***P < 0.001 compared to WT mice at the same time point.

Figure 4. Inflammatory gene expression in the retina in WT and LysM$^{Cre/+}$SOCS3$^{fl/fl}$ mice. Total RNA of WT and LysM$^{Cre/+}$SOCS3$^{fl/fl}$ mouse retina was extracted and cDNA was synthesized for real-time PCR. **A:** Messenger RNA expression of chemokines *TNF*, iNOS (official name *ISNYA1*), GMCSF (official name *CSF2*), *VEGFA*, and *Arg1* genes in normal WT and SOCS3 KO mice. **B:** mRNA expression of *TNF*, *IL1B*, iNOS, GM-CSF, *IFNG*, *IL17A*, *IL6*, *CCL2*, *CXCL2*, *VEGFA*, *IL10*, and *Arg1* genes at different stages of EAU in WT and SOCS3 KO mice. The results shown are gene fold-change compared with WT non-immunized control retina. Data are presented as Mean ± SEM. N = 6. *P < 0.05, **P < 0.01, ***P < 0.001 compared with SOCS3 KO mouse retina at the same time point. Two-way ANOVA with Bonferroni post-tests. **C, D:** Retinal flatmounts from day 60 p.i. EAU of WT (**C**) and LysM$^{Cre/+}$SOCS3$^{fl/fl}$ mice stained for CD45 (green) and arginase-1 (red) and imaged by confocal microscopy. Scale bar = 50 μm.

Figure 5. Immune gene expression and protein secretion in bone-marrow–derived macrophages (BMDMs) and neutrophils from SOCS3$^{fl/fl}$ and LysM$^{Cre/+}$SOCS3$^{fl/fl}$ mice. BMDMs were cultured from SOCS3$^{fl/fl}$ and SOCS3 KO mice and netrophils were isolated from bone marrow of these mice. Total RNA was extracted from the cells and cDNA was synthesized for real-time PCR. **A-C:** Immune gene expression in naïve non-poloarized M0 (**B**), LPS/IFNγ (**B**), or IL-4 (**C**) treated macrophages from SOCS3$^{fl/fl}$ and SOCS3 KO mice. **D:** Immune gene expression in bone-marrow–derived neutrophils from WT and SOCS3 KO mice. Data presented are gene fold-changes in cells from SOCS3 KO mice compared to that from SOCS3$^{fl/fl}$ mice under the same treatment conditions. N = 3, *P < 0.05. **E:** The protein levels in the supernatants of BMDMs from SOCS3$^{fl/fl}$ and SOCS3 KO mice under different polarization conditions. Data are presented as Mean ± SEM. N = 6. *P < 0.05; **P < 0.01. Unpaired student's *t*-test.

Figure 6. The effects of amino-2-borono-6-hexanoic (ABH) on experimental autoimmune uveoretinitis (EAU)-induced retinal angiogenesis in WT and LysM$^{Cre/+}$SOCS3$^{fl/fl}$ mice. **A, B:** LysM$^{Cre/+}$SOCS3$^{fl/fl}$ EAU mice were treated with 200 μM ABH (i.p.) or PBS once daily from day 14 to 60 p.i. **A:** Clinical score of inflammation and structural damage at days 14, 40, and 60 p.i. **B:**

Representative confocal images of retinal flatmounts from day 60 p.i. and the number of retinal neovascular membrane (RNM) in PBS- and ABH-treated SOCS3 KO mice. **C-E:** WT EAU mice were treated with 200 μM ABH (i.p.) or PBS once daily from day 60 to 79 p.i. **C:** Clinical score of inflammation and structural damage were evaluated at days 25, 60, and 80 p.i. **D:** Representative confocal images of retinal flatmounts from day 80 p.i. and the number of RNM in PBS- and ABH-treated EAU KO mice. **E:** Fluorescent angiography showing hyper-fluorescent lesions in PBS- and ABH-treated EAU mice and the average number of hyper-fluorescent lesions. Mean ± SEM, N = 5~6 mice, $*P < 0.05$, $**P < 0.01$ compared to PBS-treated group.

Table 1. Antibodies used in flow cytometry.

Target molecule	Conjugated fluorochrome	Origin	Clone	Company
CCR2	APC	Rat	475301	R&D Systems
CD8a	APC-Cy7	Rat	53-6.7	BD Biosciences
Ly6G	APC-Cy7	Rat	1A8	BD Biosciences
CX_3CR1	Alexa Fluor 488	Goat	(Polyclonal)	R&D Systems
CD4	Pacific blue	Rat	RM4-5	BD Biosciences
I/A I/E	eF450	Rat	M5/114.15.2	eBiosciences
F4/80	PE	Rat	CI:A3-1	Serotec
Gr-1	PE	Rat	RB6-8C5	BD Biosciences
CD11c	PE	Hamster	HL3	BD Biosciences
CD86	PE	Rat	GL1	BD Biosciences
CD11b	PE-Cy7	Rat	M1/70	BD Biosciences
CD45	PerCP	Rat	30-F11	BD Biosciences

Table 2. Primers used in real-time reverse transcription-PCR.

Targets	Annealing temperature (°C)	Sequences	
18S	58	Forward	5'– AGGGGAGAGCGGGTAAGAGA – 3'
		Reverse	5'–GGACAGGACTAGGCGGAACA–3'
Arg-1	61	Forward	5 – TTATCGGAGCGCCTTTCTCAA–3'
		Reverse	5'–TGGTCTCTCACGTCATACTCTGT–3'
CCL2	58	Forward	5'–AGGTCCCTGTCATGCTTCTG–3'
		Reverse	5'–TCTGGACCCATTCCTTCTTG–3'
CXCL2	58	Forward	5'–AAGTTTGCCTTGACCCTGAA–3'
		Reverse	5'–AGGCACATCAGGTACGATCC–3'
IFN-γ	56	Forward	5'–GCTCTGAGACAATGAACGCT–3'
		Reverse	5'–AAAGAGATAATCTGGCTCTGC–3'
IL-1β	58	Forward	5'–TCCTTGTGCAAGTGTCTGAAGC–3'
		Reverse	5'–ATGAGTGATACTGCCTGCCTGA–3'
IL-10	58	Forward	5'–TGCAGGACTTTAAGGGTTACTTGG–3'
		Reverse	5'–GGCCTTGTAGACACCTTGGTC–3'
IL-6	58	Forward	5'–TCTGCAAGAGACTTCCATCCAGT–3'
		Reverse	5' –TCTGCAAGTGCATCATCGTTGT–3'
iNOS	58	Forward	5'–GGCAAACCCAAGGTCTACGTT–3'
		Reverse	5'–TCGCTCAAGTTCAGCTTGGT–3'
TNF-α	58	Forward	5'–GCCTCTTCTCATTCCTGCTT–3'
		Reverse	5'–CTCCTCCACTTGGTGGTTTG–3'
VEGF-A	58	Forward	5'–CCCACGTCAGAGAGCAACAT–3'
		Reverse	5'–TTTCTTGCGCTTTCGTTTTT–3'
Ym-1	58	Forward	5'–ACTTTGATGGCCTCAACCTG–3'
		Reverse	5'–AATGATTCCTGCTCCTGTGG–3'
TGF-β	58	Forward	5'–GTGTGGAGCAACATGTGGAACT–3'
		Reverse	5'–GGGCTGATCCCGTTGATTTC–3'
IL-17a*(Il17a*)*			Mm00439618_m1
GM-CSF *(Csf2)**			Mm01290062_m1

*Gene expression was conducted using the LightCycler® 480 Probe Master from Roche Diagnostics GmbH.

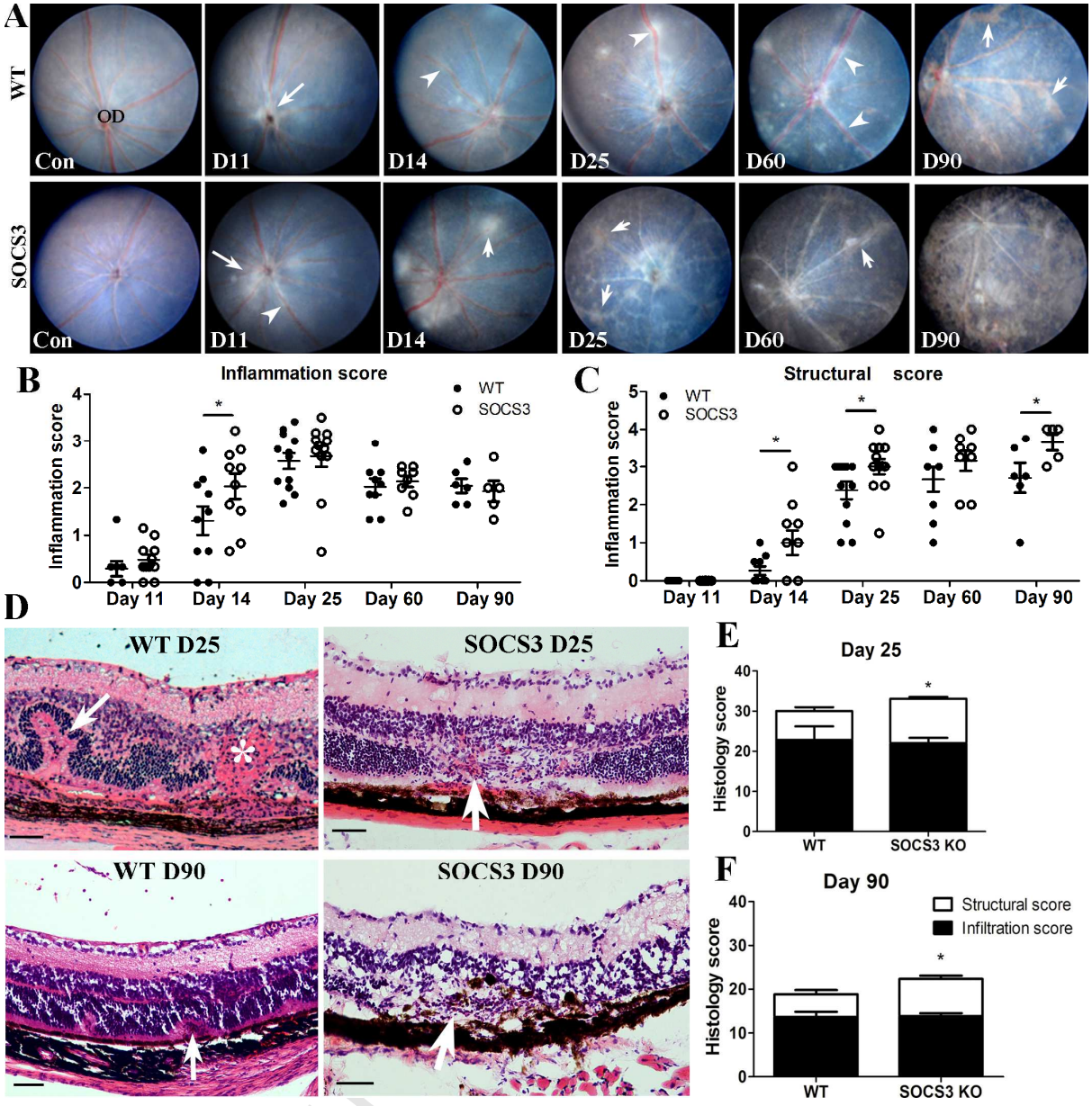
A
WT
SOCS3
OD
Con
D11
D14
D25
D60
D90
B
Inflammation score
WT
SOCS3
Day 11
Day 14
Day 25
Day 60
Day 90
C
Structural score
D
WT D25
SOCS3 D25
WT D90
SOCS3 D90
E
Day 25
Histology score
WT
SOCS3 KO
F
Day 90
Structural score
Infiltration score

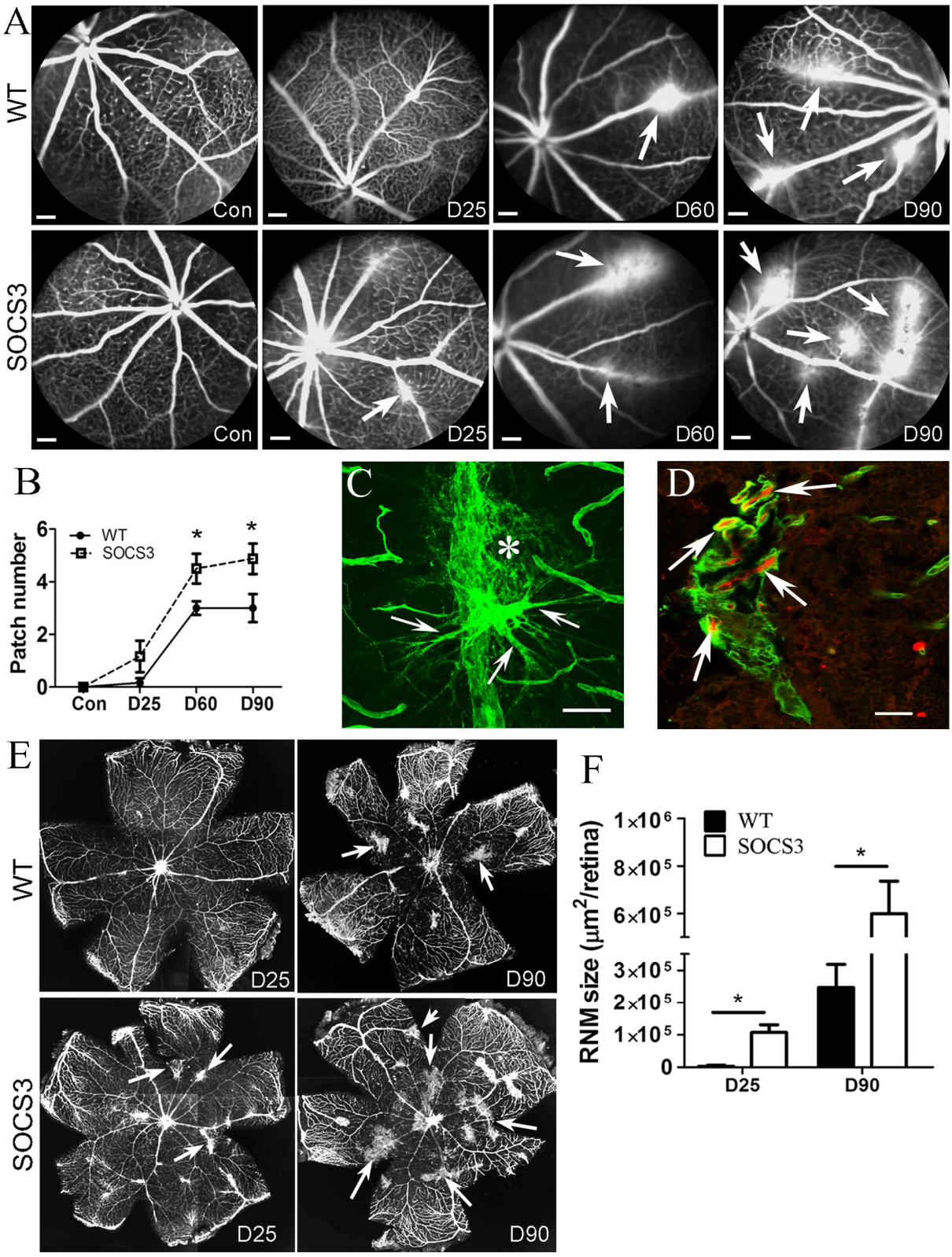
A
WT
SOCS3
Con
D25
D60
D90
B
Patch number
WT
SOCS3
Con
D25
D60
D90
C
D
E
WT
SOCS3
D25
D90
F
RNM size (μm²/retina)
WT
SOCS3
D25
D90

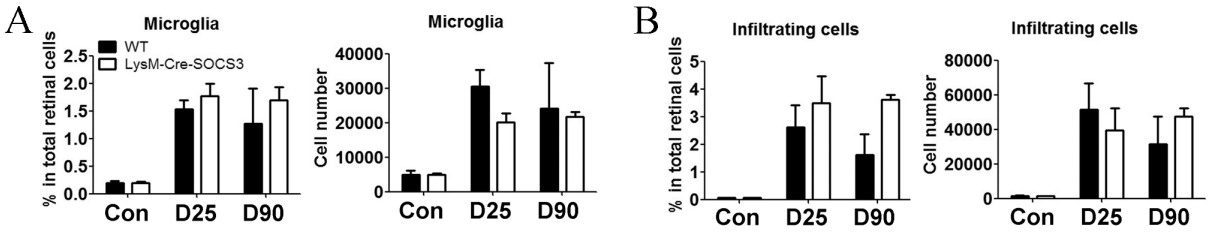

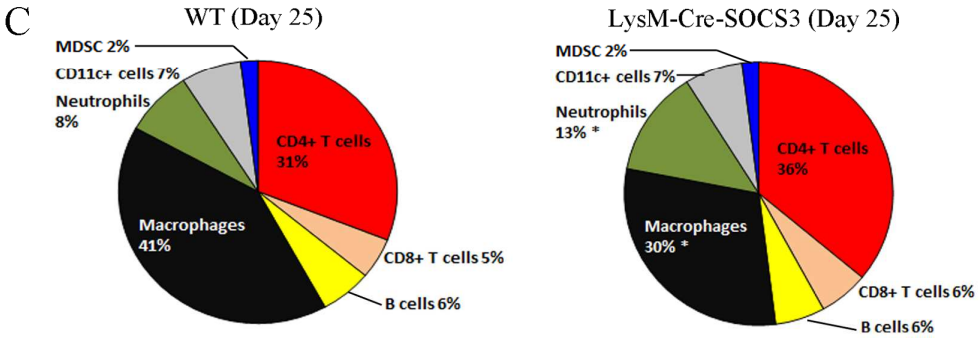

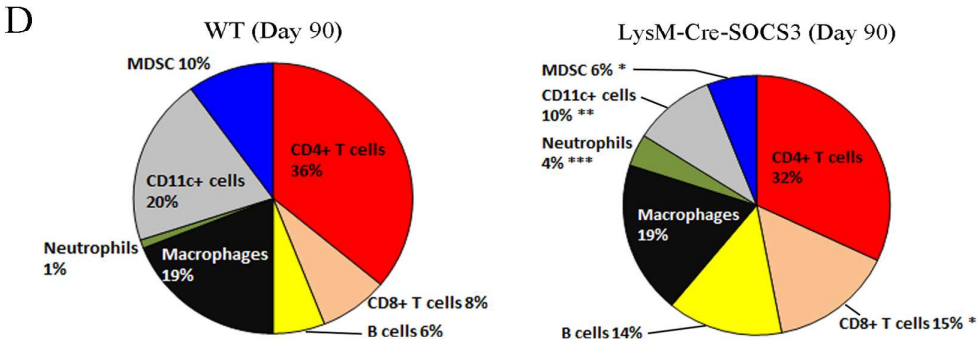

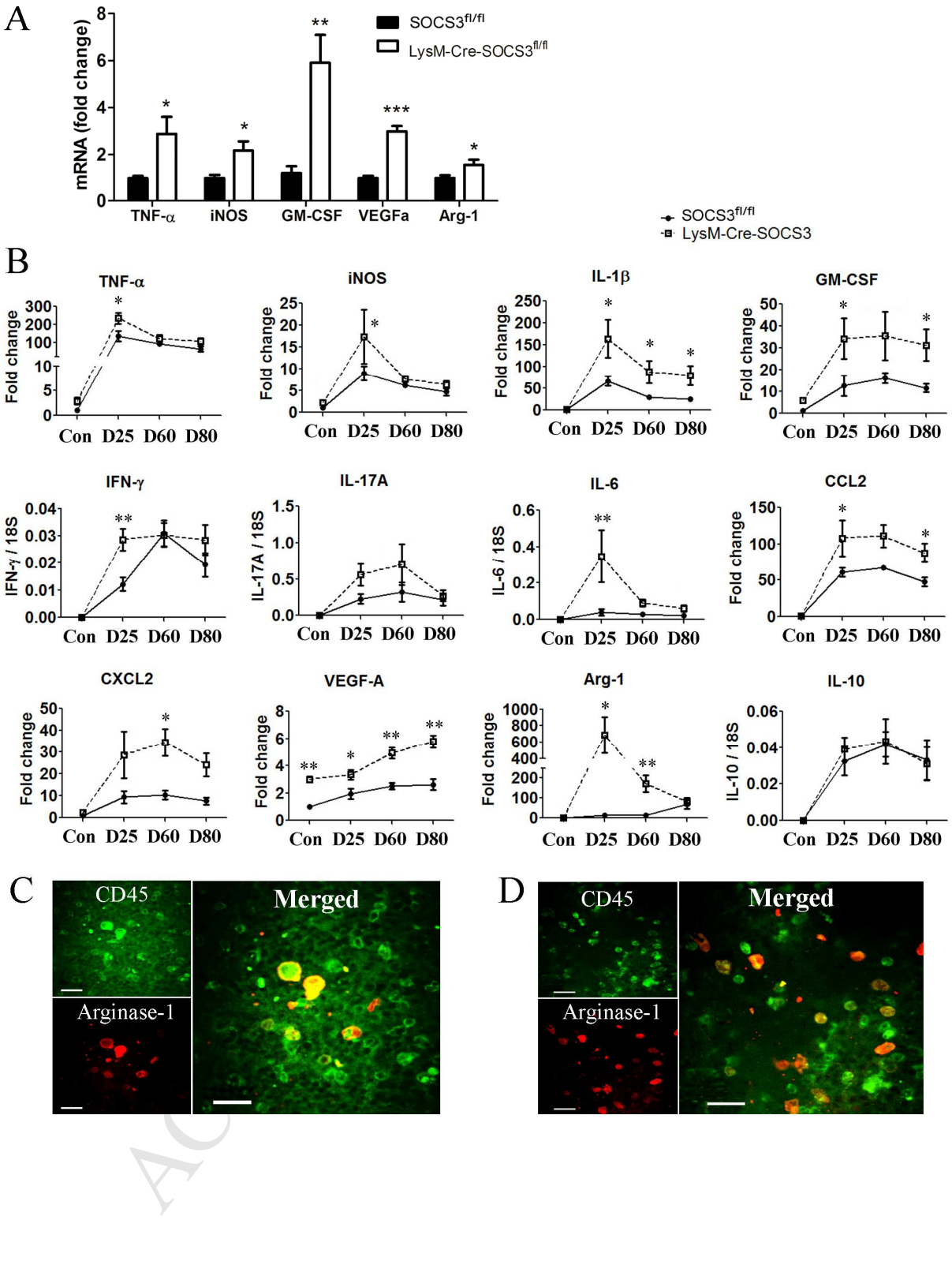
A
mRNA (fold change)
SOCS3fl/fl
LysM-Cre-SOCS3fl/fl
TNF-α
iNOS
GM-CSF
VEGFa
Arg-1
B
SOCS3fl/fl
LysM-Cre-SOCS3
TNF-α
iNOS
IL-1β
GM-CSF
IFN-γ
IL-17A
IL-6
CCL2
CXCL2
VEGF-A
Arg-1
IL-10
Fold change
IFN-γ / 18S
IL-17A / 18S
IL-6 / 18S
IL-10 / 18S
Con D25 D60 D80
C
CD45
Merged
Arginase-1
D
CD45
Merged
Arginase-1